BRAIN RESEARCH 1143 (2007) 228–237

available at www.sciencedirect.com

ScienceDirect

www.elsevier.com/locate/brainres

BRAIN RESEARCH

Research Report

Source localization of periodic sharp wave complexes using independent component analysis in sporadic Creutzfeldt–Jakob disease

Ki-Young Jung[a,*], *Dae-Won Seo*[b], *Duk L. Na*[b], *Chin-Sang Chung*[b], *Il Keun Lee*[c], *Kyungmi Oh*[a], *Chang-Hwan Im*[d], *Hyun-Kyo Jung*[e]

[a]*Department of Neurology, Korea University Medical Center, Korea University College of Medicine, #126-1, Anam-Dong 5Ga, Seongbuk-Gu, Seoul 136-705, South Korea*
[b]*Department of Neurology, Samsung Medical Center, Sungkyunkwan University School of Medicine, Seoul, South Korea*
[c]*Department of Neurology, Konkuk University School of Medicine, Seoul, South Korea*
[d]*Department of Biomedical Engineering, Yonsei University, Wonju, South Korea*
[e]*School of Electrical Engineering, Seoul National University, Seoul, South Korea*

ARTICLE INFO

Article history:
Accepted 19 January 2007
Available online 7 February 2007

Keywords:
Creutzfeldt–Jakob disease
Periodic discharge
Pathophysiology
EEG
Dipole source localization

ABSTRACT

Patients with Creutzfeldt–Jakob disease (CJD) show periodic sharp wave complexes (PSWCs) on electroencephalography (EEG) during the course of their illness. However, the source location of PSWCs and their pathophysiological mechanism remain unclear. Six patients with sporadic CJD who showed typical PSWCs on EEGs were selected for the study. Sixty epochs, each spanning the period from −0.25 to +0.25 s after the negative maximum of a typical PSWC, were selected for analysis in each patient. The EEG data matrix was decomposed using an independent component analysis based on a simple, neural network algorithm that can blindly separate mixtures of independent sources, using information maximization. The separate independent components were subjected to dipole source localization using a single dipole model. Three to seven independent components responsible for the PSWCs seen in CJD were identified. The EEG recording reconstructed from the selected independent components accounted for more than 80% of the variance in the original recording. All patients showed dipole sources responsible for the PSWCs of CJD in both the cortical and subcortical deep gray matter. In five of six patients, the dorsolateral and medial frontal cortices were the cortical sources of the PSWCs. Four patients showed dipole sources in the caudate and/or lentiform nucleus. In three patients, the dipole source was localized in the thalamus. These findings suggest that basal ganglia and thalami, as well as frontal cortices, are involved in generating PSWCs in CJD.

* *Corresponding author*. Fax: +82 2 3410 0052.
E-mail address: kyjung10@hanmail.net (K.-Y. Jung).

Abbreviations: EEG, Electroencephalography; CJD, Creutzfeldt–Jakob disease; PSWCs, Periodic spike-wave complexes; ICA, Independent component analysis

0006-8993/$ – see front matter © 2007 Elsevier B.V. All rights reserved.
doi:10.1016/j.brainres.2007.01.127

1. Introduction

Creutzfeldt–Jakob disease (CJD) is a rare and fatal neurodegenerative disease in which a rapidly progressive dementia is associated with cerebellar ataxia, diffuse myoclonus, and a variety of visual and other neurological abnormalities. The electroencephalography (EEG) pattern is distinct and changes over the course of the disease, from a pattern of diffuse and non-specific slowing to one of stereotypical high-voltage periodic sharp wave complexes (PSWCs) in an increasingly slow, low-voltage background (Fushimi et al., 2002; Wieser et al., 2004, 2006). Characteristic PSWCs are reported in 75–94% of patients with CJD (Niedermeyer and Lopes da Silva, 2004; Wieser et al., 2006). The presence of PSWCs, in association with the clinical, cerebrospinal fluid (CSF), and neuroradiological findings, is diagnostic of CJD (Kretzschmar et al., 1996). However, the pathogenesis of the PSWCs remains unknown, although cortical and subcortical mechanisms have been implicated based on a theoretical background (Gloor et al., 1968).

Dipole source localization provides information about the source location of particular EEG activities (Scherg, 1990). Pathophysiological mechanisms may also be deduced from the results of source localizations. The PSWCs in CJD are generalized discharges and may have multiple cortical sources or alternating pathways of activation in cortical areas, possibly involving a subcortical pacemaker (Neufeld and Korczyn, 1992). However, the source localization of PSWCs in CJD has not been studied.

Independent component analysis (ICA) is based on algorithms that can separate complex, multi-channel data into spatially fixed and temporally independent components (Bell and Sejnowski, 1995). Linear mixtures of the independent components form input data records, and there is no need for detailed models of the dynamics or spatial structure of the separated components. Even if two processes occur simultaneously, ICA can be used to separate them (Kobayashi et al., 1999).

Recently, using source localization of the independent components determined by ICA, we found that only a few sources were responsible for the generalized, apparently synchronous, epileptiform discharges, which may have different orientations and source locations (Jung et al., 2005). In the same way, a combined method using ICA and dipole source localization may be useful in defining sources of generalized discharges such as PSWCs in CJD.

The aims of this study were to identify the source location of PSWCs using combined ICA and dipole source localization and to identify the pathophysiological mechanisms of PSWCs in CJD. To do this, we applied ICA to PSWC data obtained from EEGs, analyzed the characteristic spatiotemporal patterns of the independent components, and localized the sources of the independent components, using single-dipole source estimation. To characterize the dipole source responsible for PSWCs across the patients, we performed cluster analysis using the K-means algorithm. We found a few sets of dipole clusters among the patients and sought to explain the pathophysiological mechanism(s) of PSWCs based on these results.

2. Results

2.1. Patients and clinical characteristics

Six patients (4 men, 2 women) were included in this study; their mean age was 67.0±3.4 years (range, 63–72 years). EEGs were performed one to three times in each patient (mean, 2.3±1.0). The mean interval between the onset of disease and the appearance of PSWCs on EEG was 14±16.7 weeks (range, 4–48 weeks). Progressive memory deficit and gait disturbance were the most common initial symptoms. All patients suffered from akinetic mutism and generalized myoclonus by the time the PSWCs became apparent on EEG (Table 1). One patient (no. 6) suffered from visual hallucinations.

The mean interval from scanning brain MRI to EEG recordings showing PSWCs was 14.8±10.8 days. Brain MRI showed no abnormalities in three patients. One patient (no. 6) showed high-signal lesions on T2-weighted and fluid-attenuated inversion recovery (FLAIR) images, involving multiple cortical and subcortical structures, including the cingulate, insula, temporal, and occipital cortices; the caudate; and the putamen. Two patients (nos. 4 and 5) showed subtle high-signal lesions on T2-weighted and FLAIR images in the bilateral caudate nuclei.

2.2. ICA and dipole source localization

Sixty 0.5-s epochs spanning the period from −0.25 to +0.25 s after the negative maximum of the typical PSWC were selected from whole EEG recordings in each patient. These were subsequently concatenated to construct an EEG data matrix that was used for the ICA (Fig. 1A). As EEG was conducted using 21 channels, 21 independent components were decomposed from each EEG dataset (Figs. 1B, C). The mean number of independent components to reach a "percent variance accounted for" (PVAF) of more than 80% was 4.8±1.5 (range, 3–7) in each patient (Fig. 2). As a result, 29 independent components from six patients were further analyzed. The

Table 1 – Clinical status of the patients

Patient no.	Age (years)	Sex	Clinical manifestation at the time of EEG recording	Interval to PSWCs (weeks)
1	63	M	Akinetic mutism, R hemiparesis, myoclonus	12
2	66	M	Rigidity, myoclonus	48
4	72	M	Gait disturbance, poor oral intake, myoclonus	4
5	66	M	Dysequilibrium, rigidity, myoclonus	12
6	65	F	Gait disturbance, memory deficit, visual hallucinations, myoclonus	4
10	70	F	Insomnia, agitation, rigidity, myoclonus	8

PSWCs: Periodic sharp wave complexes, M: Male, F: Female.

mean residual variance of the fitted dipoles for each selected independent component was 6.3±2.3%.

All patients showed dipole sources responsible for the PSWCs of CJD in both the cortical and subcortical deep gray matter (Fig. 3, Table 2). In four patients, we observed sources in the dorsolateral frontal region, including the superior, middle, and inferior frontal gyrus. In four patients, we observed sources in the medial frontal regions, such as the medial frontal gyrus and cingulate cortex; dipole sources were in both the dorsolateral and medial frontal regions in three of these patients. One patient (no. 6), with visual hallucinations, had two dipole sources in both occipital cortices (left lingual gyrus and right cuneus). A source was observed in the insular cortex in one patient (no. 5). The caudate nucleus, lentiform nucleus, and thalamus were the locations of the subcortical structures. Four patients showed dipole sources in the caudate and/or lentiform nucleus. In three patients, the dipole source was localized in the thalamus. One patient (no. 1) had dipole sources in both the caudate nucleus and thalamus.

2.3. *Clustering dipole sources across the patients*

Defining multiple clusters that represent relatively common EEG activities across subjects and examining the nature of subject differences within and between clusters allows detailed exploration of subject EEG differences (Onton and Makeig, 2006; Onton et al., 2006). Dipole sources located in proximity to each other were classified into the same subsets (clusters), according to the distance measured in vector space using the K-means algorithm. The dipoles in each cluster may share common traits. Seven clusters of dipole sources were classified from the 29 components responsible for PSWCs across the six CJD patients (Fig. 4). Because the K-means algorithm does not consider the orientation of the dipole but only the distance among dipole sources, the scalp map of each dipole has a slightly different topographic pattern in a given cluster (Fig. 4). Three dipoles located in the deep white matter, subgyral gray, and insular cortex were classified as outliers, because the locations of the sources were far (>2.5 S.D.) from the other dipoles.

Four distinct groups of clusters were identified according to the homotopic anatomical locations between both hemispheres. Clusters 5, 7, and 3 represented cortical sources of PSWCs in CJD patients (Fig. 4). The blue dots in clusters 5 and 7 show subsets of dipole sources in the dorsolateral and medial frontal region, respectively, and the red dots indicate the centroid of the blue dots in Fig. 4. Cluster 5 consisted of three components from two patients, and cluster 6 involved six components from four patients. Cluster 3 revealed two dipole sources, located in the occipital cortices, in patient no. 6. Clusters 6, 8, and 4 involved subcortical sources, including the caudate, lentiform nuclei, and thalami. Clusters 6 and 8 demonstrated dipole sources from both the caudate and lentiform nuclei from five patients. In three patients, cluster 4 was the thalamic source in either hemisphere.

3. Discussion

We attempted to identify the location of dipole sources responsible for the PSWCs in CJD. Both cortical and subcortical areas accounted for the generalized periodic discharges. In five of six patients, the dorsolateral and medial frontal cortices were the cortical sources of the PSWCs. The basal ganglia and thalamus were the subcortical locations.

The medial and dorsolateral frontal regions are frequently involved in producing generalized epileptiform discharges in generalized epilepsy (Holmes et al., 2004; Rodin, 1999). In addition, only a few dipole sources could explain the generalized discharges of absence epilepsy (Jung et al., 2005; McKeown et al., 1999; Meeren et al., 2005; Rodin et al., 1994) and of juvenile myoclonic epilepsy (Santiago-Rodriguez et al., 2002). Experimental electron microscopy evidence in CJD has shown that fusions of cortical neuronal processes can lead to abnormal electronic coupling between cells, whereby large neuronal aggregates burst with near synchrony, resulting in generalized synchronized discharges (Traub and Pedley, 1981). Thus, the frontal cortices may participate in producing generalized discharges in CJD.

Dipole sources accounting for PSWCs in CJD were located in the subcortical deep gray matter, in addition to the cortical sources. All of the patients had source locations in the caudate/lentiform nuclei and/or thalamus. Four patients had dipole sources in the caudate and/or lentiform nuclei. Signal changes in the caudate and putamen are characteristic findings on MRI in CJD patients (Tschampa et al., 2005; Urbach et al., 1998). Depth electrodes in the caudate nucleus have shown that the PSWCs in CJD arose from subcortical sources (Chiofalo et al., 1980). Thus, we speculate that the caudate nucleus is an important source for generating PSWCs in CJD.

The thalamocortical system has been implicated in producing generalized spike-wave discharges (GSWDs) in absence epilepsy (McCormick and Contreras, 2001). Here, dipole source localization showed that the thalamus was involved in three patients. Tschampa and colleagues reported that the inspection of brain MR images, using apparent diffusion coefficients, revealed thalamic involvement in most CJD patients (Tschampa et al., 2003). Neuropathological data also suggest that the numbers of thalamus and brainstem neuronal cells decrease in the early stages of CJD (Iwasaki et al., 2005; Tschampa et al., 2002). In addition, damage to thalamic neurons has been associated with PSWCs (Tschampa et al., 2002; Zochodne et al., 1988). These findings are consistent with the thalamus playing a role in the production of PSWCs in CJD.

Experimental data suggest that basal ganglia circuits, including cortico-striatal and cortico-subthalamo-pallidal networks, participate in the control of abnormal oscillations in the thalamocortical loop (Paz et al., 2005; Slaght et al., 2004). Frontal intermittent rhythmic delta activity (FIRDA) and triphasic wave-like activities are recognized as forerunners of PSWCs (Hansen et al., 1998; Wieser et al., 2004) and are observed when cortical and subcortical gray matter are involved (Gloor et al., 1968). Severe impairment of cortical–subcortical structures is also necessary for subacute sclerosing panencephalitis complexes, which may be analogous to the PSWCs of CJD (Celesia, 1973). Thus, the basal ganglia and thalamus may have a supplementary role in the production of PSWCs in CJD. Considering all these results, we hypothesize that a subcortical mechanism in combination with cortical sources is involved in

generating the generalized periodic discharges in CJD. This is consistent with the results of Gloor and colleagues (Gloor et al., 1968). Further experimental studies using animal model are needed to examine this.

Statistical analyses using the clustering method are consistent with both frontal cortices and subcortical nuclei being the regular dipole sources accounting for PSWCs in CJD patients. All patients showed akinetic mutism, myoclonus, generalized rigidity, and variable degrees of impaired consciousness, including drowsiness and confusion. Akinetic mutism and myoclonus may be associated with frontal lobe dysfunction. Lesions in the basal ganglia can cause rigidity, and thalamic dysfunction may contribute to impaired consciousness. These clinical manifestations may relate to dipole sources in the frontal cortices and subcortical structures. Remarkably, one patient with visual hallucination (no. 6) had

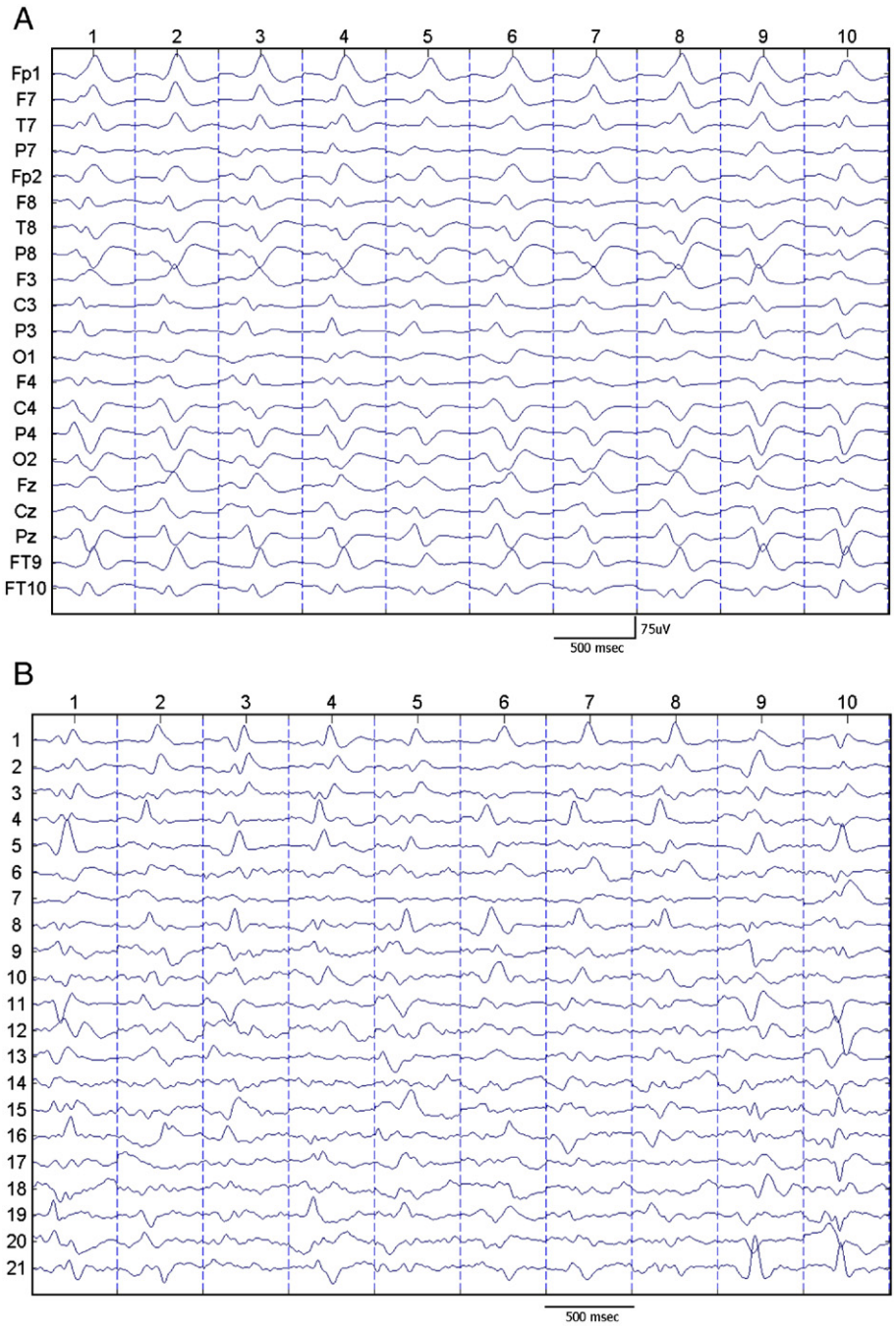

Fig. 1 – (A) Concatenated EEG data (patient no. 6), composed of 30 0.5-s epochs. A single epoch is defined as EEG data spanning the period from −0.25 to +0.25 s after the negative maximum of a typical PSWC. Only 10 epochs are presented in this figure. Activation wave forms (B) and scalp topographic map (C) of the resulting 21 components separated by ICA in the same patient. PSWCs: Periodic sharp wave complexes, ICA: Independent component analysis.

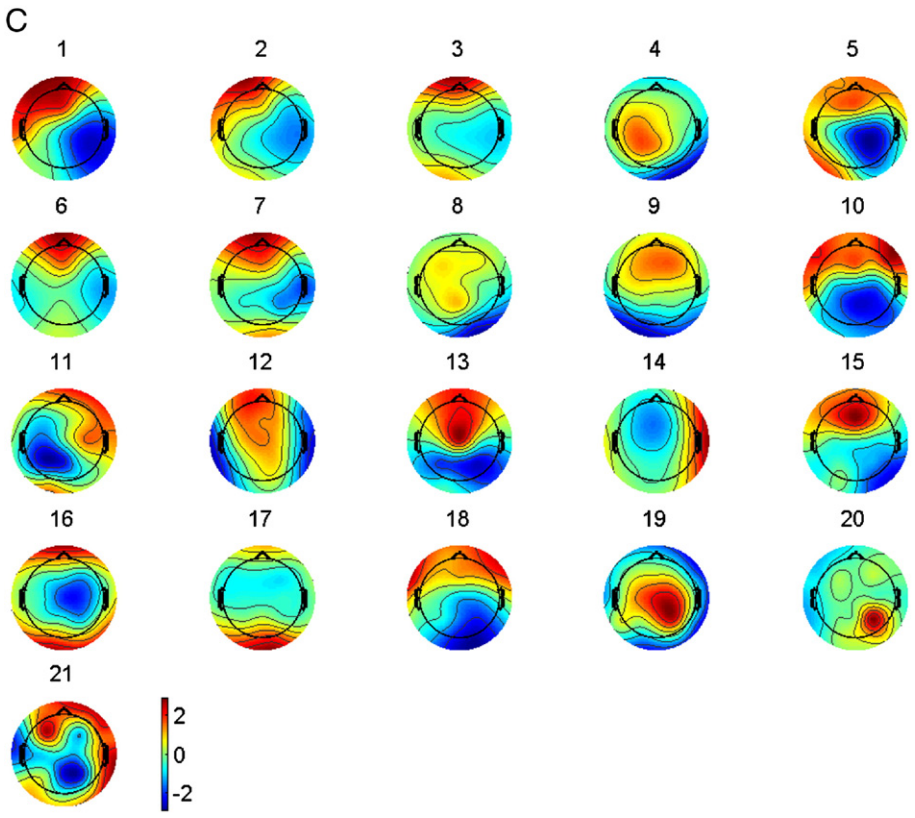

Fig. 1 (*continued*).

dipole sources in both occipital cortices, in addition to the subcortical nuclei. Dipole source localization of PSWCs in CJD appears to be in line with clinical symptomatology. However, it is necessary to evaluate relationships between source locations of EEG activity and clinical manifestations in a large patient group, according to disease stage.

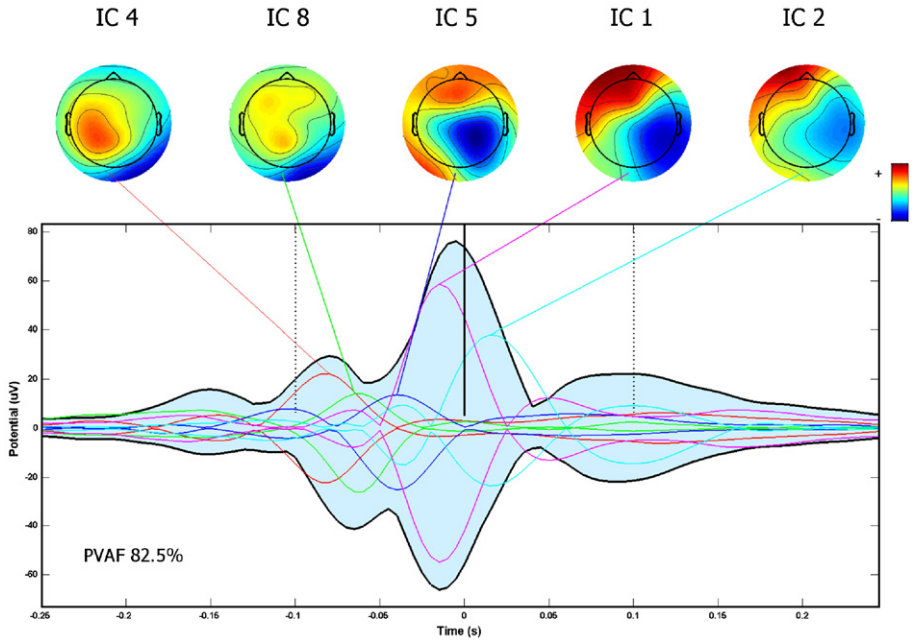

Fig. 2 – Identifying independent components accounting for PSWCs using an envelope map in EEGLAB (patient no. 6, as in Fig. 1). Five (1, 2, 4, 5, and 8) of the 21 components account for 82.5% of PSWCs. PVAF: Percent variance accounted for PSWCs, PSWCs: Periodic sharp wave complexes.

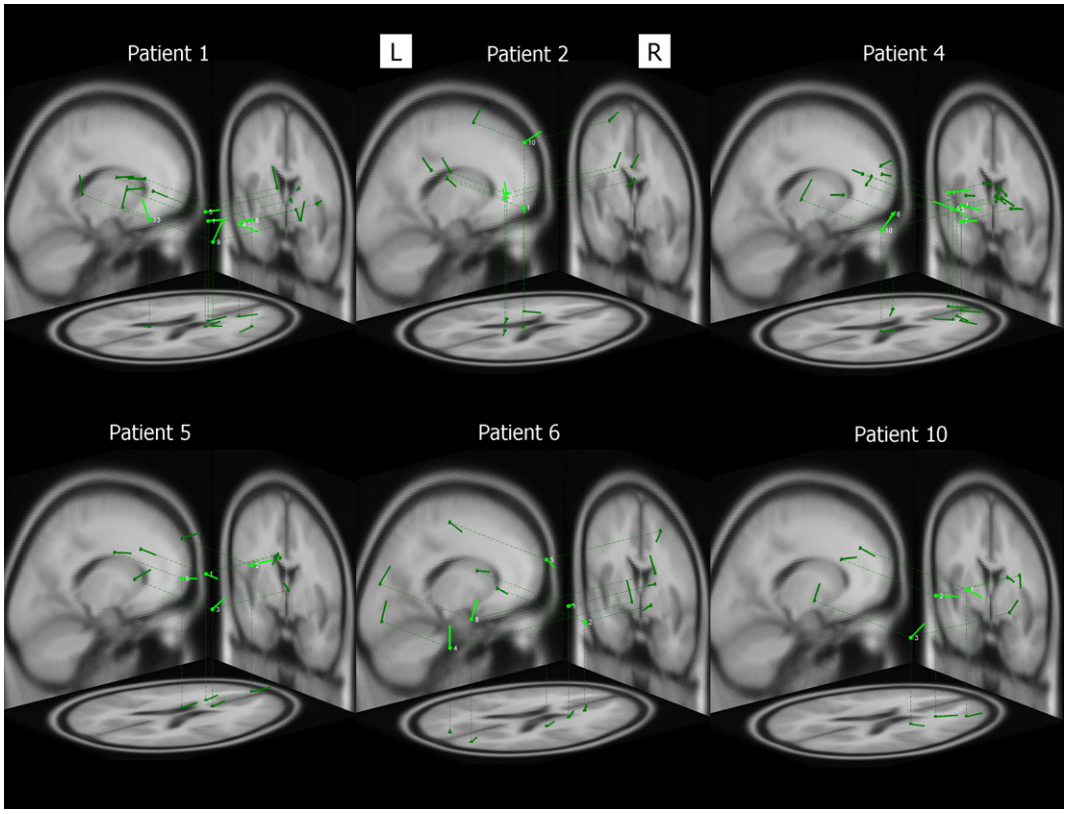

Fig. 3 – Localization of independent components responsible for PSWCs in each patient as a single dipole source on a standard MRI template. PSWCs: Periodic sharp wave complexes.

Although PSWCs in CJD are similar to the GSWD of idiopathic generalized epilepsy in terms of distribution and morphology of discharges by visual inspection, we found differences between the two by source localization using ICA. The number of independent components accounting for PSWCs in each patient ranged from three to seven. Although the distribution of PSWCs in CJD was generalized, only a few cortical and subcortical sources were responsible for the generalized discharges in CJD, as was true for the GSWD of generalized epilepsy. However, it seems that the number of sources required to explain periodic generalized discharges was slightly higher than previously reported in generalized epilepsy (Jung et al., 2005; McKeown et al., 1999; Santiago-Rodriguez et al., 2002). All of the patients in our study showed a markedly asymmetric distribution of dipole sources, in contrast to the fairly symmetric distribution between the hemispheres seen in generalized epilepsy. These findings suggest that, in contrast to generalized epilepsy, CJD shows more widespread and heterogeneous involvement during the disease process.

We used the localization of independent components, decomposed by ICA, as a single dipole source. Discrete sources of neural activity add linearly to form the observed electrical activity recorded using scalp electrodes. In other words, each scalp electrode records a weighted mixture of different cortical sources by volume conduction. Furthermore, the activities of the cortical EEG sources can be concurrently modulated by more than one process (Delorme and Makeig, 2004). Thus, applying the source localization method to raw EEG data could erroneously localize sources, which inevitably contain artifacts and extracerebral activities in addition to the brain signals of interest. It is more accurate to localize sources pertaining to only brain activities after separating EEG data into maximally independent components.

ICA algorithms can separate complex multi-channel data into spatially fixed and temporally independent components, linear mixtures of which form the input data records, without detailed models of either the dynamics or spatial structure of the separated components (Delorme and Makeig, 2004). The mathematical idea behind ICA is to minimize mutual information among the data projections. As decomposed components produced by ICA are maximally temporally independent and spatially fixed, each independent component has its own scalp voltage topographic distribution. Thus, the independent components that have been selected could be used for a single dipole source in a head model. The usefulness of source localization of independent components in the dipole model and current density reconstruction after ICA has recently been demonstrated (Barbati et al., 2006; Jung et al., 2005; Kobayashi et al., 2001; Marco-Pallares et al., 2005).

To our knowledge, the source localization of PSWCs in CJD has not been studied previously. Our results suggest that both subcortical and cortical mechanisms are involved in generating PSWCs in CJD. Source localization with EEG may help

Table 2 – Summary of EEG source localization and MRI findings

Patient no.	IC #	Location of dipole source	Talairach coordinate			RV (%)	Sum of PVAF (%)
			x	*y*	*z*		
1	1	R caudate nu.	7	10	5	1.2	82.6
	4	R med. fr. gy.	13	34	−2	11.0	
	5	R caudate n.	16	0	16	4.7	
	6	R inf. fr. gy.	37	27	9	13.0	
	9	R lentiform nu.	18	5	−6	13.0	
	13	L thalamus	−10	−32	12	14.0	
2	1	R thalamus	1	−16	20	8.1	83.5
	2	L cingulate	−2	−30	29	6.0	
	3	L deep WM	−23	−12	24	9.0	
	10	L mid. fr. gy.	−29	11	54	12.0	
4	1	L ACC	−12	23	23	2.6	81.7
	2	L sup. fr. gy.	−7	62	21	2.3	
	3	R caudate nu.	3	16	3	5.7	
	5	L cingulated	−9	−1	27	3.0	
5	1	L med. fr. gy.	−10	55	12	7.8	81.0
	3	R med. fr. gy.	11	46	7	4.0	
	4	R med. fr. gy.	4	56	6	5.7	
	5	R ACC	16	38	11	5.7	
	6	L insula	−31	20	0	7.7	
	7	R ACC	22	41	2	5.3	
	10	R thalamus	4	−19	6	5.5	
6	1	R caudate nu.	18	8	12	2.2	82.5
	2	R caudate nu.	13	26	−4	4.3	
	4	L lingual gy.	−9	−81	−2	3.1	
	5	R subgyral gy.	24	−16	53	11.0	
	8	R cuneus	18	−81	25	7.8	
10	1	R mid. fr. gy.	34	40	21	5.1	81.0
	2	R caudate nu.	20	22	18	3.9	
	3	L lentiform nu.	22	−4	−5	5.5	

IC #: Independent component number, RV: Residual variance, B: Bilateral, L: Left, R: Right, nu.: Nucleus, fr.: Frontal, gy.: Gyrus, med.: Medial, sup.: Superior, mid.: Middle, inf.: Inferior, WM: White matter, ACC: Anterior cingulate cortex, PVAF: Percent variance of sum of the independent components accounting for periodic sharp wave complexes.

elucidate the pathophysiological mechanisms as well as provide information about the anatomical location itself.

4. Experimental procedures

4.1. *Patients*

Ten patients were consecutively diagnosed with sporadic CJD between 1995 and 2000 at the Samsung Medical Center. The diagnoses were based on pathology (2 patients) or clinical and EEG findings, according to diagnostic criteria (Kretzschmar et al., 1996). CSF 14-3-3 protein data were not available for all patients. Six patients showing typical PSWCs with generalized symmetric distribution on EEG were selected in the present study. Four patients were excluded for the following reasons: digital EEG was not available for one patient, one patient showed no typical PSWCs but did demonstrate some features of periodic patterns, and two patients had only lateralized periodic discharges in the left hemisphere. Both T1- and T2-weighted MR images were obtained for all patients.

4.2. *EEG recordings*

Routine EEG recordings were obtained for at least 30 min from each patient, while awake and sleeping, using a 32-channel digital EEG machine (Vanguard system, Cleveland Clinic Foundation Healthcare Ventures, Inc., Cleveland, OH). The EEG recordings were made using 21 electrodes (Fp1, F7, T7, P7, F3, C3, P3, O1, Fp2, F8, T8, T8, F4, C4, P4, O2, Fz, Cz, Pz, FT9, and FT10) placed on the scalp according to the international 10–20 system, with reference to the Pz electrode. Electrode impedance was maintained at less than 5 kΩ. The band pass filter setting was 0.5–70.0 Hz, with a sampling rate of 200 Hz.

PSWCs were defined as a sharp wave or sharp bi- or triphasic complexes of 100 to 500 ms in duration, with 500- to 2000-ms intervals between complexes and with a stable repetition rate and monomorphic configuration in the same derivation (Steinhoff et al., 1996). Patients with EEG findings of frontal intermittent rhythmic delta activity, lateralized periodic patterns, or triphasic wave-like periodic patterns without PSWCs were excluded from the study.

4.3. *ICA and selection of relevant component*

All recorded data were reviewed for technical and biological artifacts. To select similar epochs, we used a spatiotemporal pattern search that used the information from all channels for the marked epoch in the BESA program (Scherg et al., 2002). After marking an epoch spanning the period from −0.25 to +0.25 s after the negative maximum of a typical PSWC by visual inspection, a single channel having the highest amplitude was selected as a transient search template. The marked pattern in the selected channel was searched, and an average waveform was generated from a few PSWCs. Then, this initial average was used as a template, and all segments having a spatiotemporal correlation greater than 85% with the average template were identified. Sixty 0.5-s epochs were selected for analysis; these epochs were concatenated to construct an EEG data matrix that was used for the ICA (Fig. 1A).

The EEG data matrix was decomposed using an ICA algorithm based on a simple, neural network algorithm that could blindly separate mixtures of independent sources, using information maximization (Bell and Sejnowski, 1995). We used an open-source ICA program (EEGLAB version 5.03; Delorme and Makeig, 2004) and operated in the MATLAB environment (version 7.01, MathWorks, Natick, MA). The ICA algorithm was applied, and it produced 21 independent components. The components accounting for the PSWCs were selected according to literature procedures (Onton et al., 2005). Initially, the decomposed component activations were plotted temporally (Fig. 1B) and mapped spatially to scalp topography (Fig. 1C). Independent components of extracerebral origin, including muscle artifacts, eye movements, and 60 Hz noises, were excluded by visual inspection of scalp voltage topography and activation spectra. Then, after conducting single dipole source localization for each independent component using the DIPFIT function of EEGLAB (see below), components of that dipole source located outside the head model or with a residual variance of more than 15% were further excluded (Onton et al., 2005). Each remaining component was back projected, and scalp potential was recon-

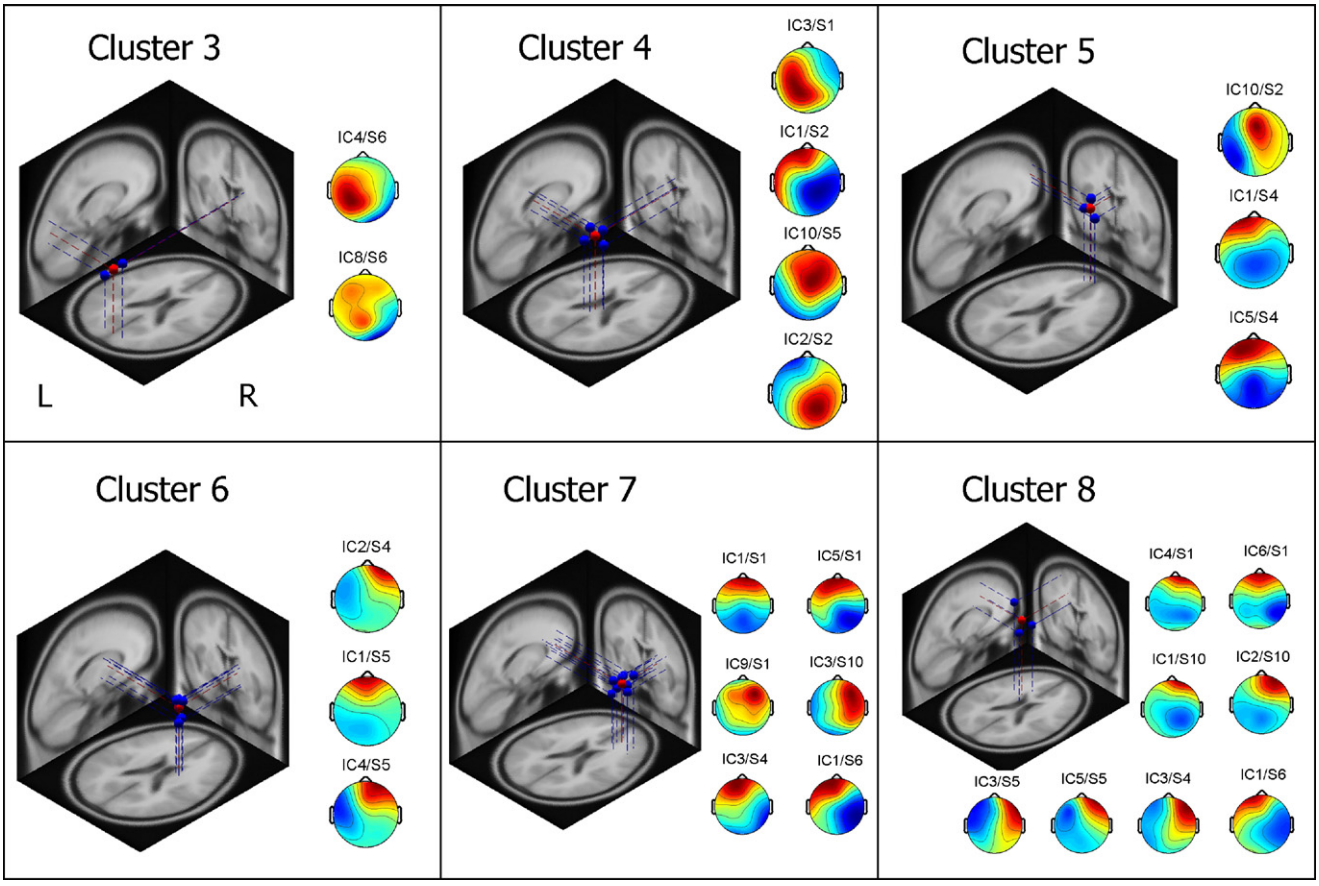

Fig. 4 – Cluster analysis using the K-means algorithm showed seven clusters of dipole sources, including an outlier (not shown). Blue dots indicate individual independent components, and red dots indicate the centroid of clustered components in a given cluster. Four distinct clusters (apart from an outlier) are noted, if the homotopic anatomical location between both hemispheres is taken into consideration. Clusters 5 and 7 represent dipole sources in the medial and dorsolateral frontal cortices. Cluster 3 shows dipole sources in the occipital region. Clusters 6 and 8 reveal dipole sources located in the caudate and lentiform nuclei. Cluster 4 indicates thalamic sources. Scalp map of individual independent component in each cluster is also presented. (For interpretation of the references to colour in this figure legend, the reader is referred to the web version of this article.)

structed, for comparison with the original EEG. The component(s) behaviorally most relevant to the PSWCs of the original EEG in the time period between −100 ms and +100 ms were selected from the remaining components, using an envelope topographic map (Fig. 2). The degree of relevance of the component(s) to the original EEG was estimated by calculating 'percent variance accounted for' (PVAF) as follows: 100×[1−variance(original EEG−reconstructed EEG)÷variance(original EEG)], where reconstructed EEG means the EEG data resulting from reconstructing one or more independent component(s) responsible for PSWCs (Delorme and Makeig, 2004). The independent components were selected in order, starting from the component with the highest PVAF value, until the sum of the PVAFs for the selected components was more than 80%.

4.4. *Dipole source localization*

A single equivalent dipole source model was used for each independent component selected. We used the DIPFIT function in EEGLAB, which uses a non-linear fitting of a single dipole model, to explain the scalp potential distribution (Scherg, 1990). The source location was estimated within a four-shell, spherical model of the head. For the head model, we assumed conductivities (mhos/m) of 0.33, 0.0042, 1.00, and 0.33 for the scalp, skull, CSF, and brain, respectively. The radii of the spheres were standardized to 85, 79, 72, and 71 mm, respectively. Transposition of the dipole location from the spherical head model to the average MRI template was included in the DIPFIT function, by co-registering the Montreal Neurological Institute (MNI) average brain image with the electrode landmark positions (http://www.sccn.ucsd.edu/eeglab/dipfittut/dipfit.html). Then, the anatomical location of the fitted source was defined using the Talairach Daemon client (version 1.1) with 7 mm of cube search range (Research Imaging Center, University of Texas Health Science Center, San Antonio, TX) (Lancaster et al., 2000).

4.5. *Cluster analysis*

Dipole sources having similar spatial locations were clustered using the K-means algorithm, implemented in EEGLAB. The K-

means algorithm clusters objects into k partitions based on attributes (MacQueen, 1967). The algorithm starts by partitioning the input points into k initial sets. The algorithm then assigns the observations into various clusters to minimize the total within-class sum of squares. We set 12 as an initial k and 2.5 S.D. for the cut-off of outliers. After inspection of the initial clustering result, the k value was adjusted stepwise until the resulting clusters were stable and anatomically plausible. The final k was 7.

REFERENCES

Barbati, G., Sigismondi, R., Zappasodi, F., Porcaro, C., Graziadio, S., Valente, G., Balsi, M., Rossini, P.M., Tecchio, F., 2006. Functional source separation from magnetoencephalographic signals. Hum. Brain Mapp. 27 (12), 925–934.

Bell, A.J., Sejnowski, T.J., 1995. An information-maximization approach to blind separation and blind deconvolution. Neural Comput. 7 (6), 1129–1159.

Celesia, G.G., 1973. Pathophysiology of periodic EEG complexes in subacute sclerosing panencephalitis (SSPE). Electroencephalogr. Clin. Neurophysiol. 35 (3), 293–300.

Chiofalo, N., Fuentes, A., Galvez, S., 1980. Serial EEG findings in 27 cases of Creutzfeldt–Jakob disease. Arch. Neurol. 37 (3), 143–145.

Delorme, A., Makeig, S., 2004. EEGLAB: an open source toolbox for analysis of single-trial EEG dynamics including independent component analysis. J. Neurosci. Methods 134, 9–21.

Fushimi, M., Sato, K., Shimizu, T., Hadeishi, H., 2002. PLEDs in Creutzfeldt–Jakob disease following a cadaveric dural graft. Clin. Neurophysiol. 113 (7), 1030–1035.

Gloor, P., Kalabay, O., Giard, N., 1968. The electroencephalogram in diffuse encephalopathies: electroencephalographic correlates of grey and white matter lesions. Brain 91, 779–802.

Hansen, H.C., Zschocke, S., Sturenburg, H.J., Kunze, K., 1998. Clinical changes and EEG patterns preceding the onset of periodic sharp wave complexes in Creutzfeldt–Jakob disease. Acta Neurol. Scand. 97 (2), 99–106.

Holmes, M.D., Brown, M., Tucker, D.M., 2004. Are "generalized" seizures truly generalized? Evidence of localized mesial frontal and frontopolar discharges in absence. Epilepsia 45 (12), 1568–1579.

Iwasaki, Y., Hashizume, Y., Yoshida, M., Kitamoto, T., Sobue, G., 2005. Neuropathologic characteristics of brainstem lesions in sporadic Creutzfeldt–Jakob disease. Acta Neuropathol. (Berl.) 109 (6), 557–566.

Jung, K.Y., Kim, J.M., Kim, D.W., Chung, C.S., 2005. Independent component analysis of generalized spike-and-wave discharges: primary versus secondary bilateral synchrony. Clin. Neurophysiol. 116 (4), 913–919.

Kobayashi, K., James, C.J., Nakahori, T., Akiyama, T., Gotman, J., 1999. Isolation of epileptiform discharges from unaveraged EEG by independent component analysis. Clin. Neurophysiol. 110 (10), 1755–1763.

Kobayashi, K., Merlet, I., Gotman, J., 2001. Separation of spikes from background by independent component analysis with dipole modeling and comparison to intracranial recording. Clin. Neurophysiol. 112 (3), 405–413.

Kretzschmar, H.A., Ironside, J.W., DeArmond, S.J., Tateishi, J., 1996. Diagnostic criteria for sporadic Creutzfeldt–Jakob disease. Arch. Neurol. 53 (9), 913–920.

Lancaster, J.L., Woldorff, M.G., Parsons, L.M., Liotti, M., Freitas, C.S., Rainey, L., Kochunov, P.V., Nickerson, D., Mikiten, S.A., Fox, P.T., 2000. Automated Talairach atlas labels for functional brain mapping. Hum. Brain Mapp. 10 (3), 120–131.

MacQueen, J.B., 1967. Some methods for classification and analysis of multivariate observations. Proceedings of 5th Berkeley Symposium on Mathematical Statistics and Probability. University of California Press, Berkeley, pp. 281–297.

Marco-Pallares, J., Grau, C., Ruffini, G., 2005. Combined ICA-LORETA analysis of mismatch negativity. NeuroImage 25 (2), 471–477.

McCormick, D.A., Contreras, D., 2001. On the cellular and network bases of epileptic seizures. Annu. Rev. Physiol. 63, 815–846.

McKeown, M.J., Humphries, C., Iragui, V., Sejnowski, T.J., 1999. Spatially fixed patterns account for the spike and wave features in absence seizures. Brain Topogr. 12 (2), 107–116.

Meeren, H., van Luijtelaar, G., Lopes da Silva, F., Coenen, A., 2005. Evolving concepts on the pathophysiology of absence seizures: the cortical focus theory. Arch. Neurol. 62 (3), 371–376.

Neufeld, M.Y., Korczyn, A.D., 1992. Topographic distribution of the periodic discharges in Creutzfeldt–Jakob disease (CJD). Brain Topogr. 4 (3), 201–206.

Niedermeyer, E., Lopes da Silva, F., 2004. Electroencephalography: Basic Principles, Clinical Applications, and Related Fields. Lippincott Williams and Wilkins, Philadelphia.

Onton, J., Makeig, S., 2006. Chapter 7 Information-based modeling of event-related brain dynamics. Prog. Brain Res. 159, 99–120.

Onton, J., Delorme, A., Makeig, S., 2005. Frontal midline EEG dynamics during working memory. NeuroImage 27 (2), 341–356.

Onton, J., Westerfield, M., Townsend, J., Makeig, S., 2006. Imaging human EEG dynamics using independent component analysis. Neurosci. Biobehav. Rev. 30 (6), 808–822.

Paz, J.T., Deniau, J.M., Charpier, S., 2005. Rhythmic bursting in the cortico-subthalamo-pallidal network during spontaneous genetically determined spike and wave discharges. J. Neurosci. 25 (8), 2092–2101.

Rodin, E., 1999. Decomposition and mapping of generalized spike-wave complexes. Clin. Neurophysiol. 110 (11), 1868–1875.

Rodin, E.A., Rodin, M.K., Thompson, J.A., 1994. Source analysis of generalized spike-wave complexes. Brain Topogr. 7 (2), 113–119.

Santiago-Rodriguez, E., Harmony, T., Fernandez-Bouzas, A., Hernandez-Balderas, A., Martinez-Lopez, M., Graef, A., Carlos Garcia, J., Fernandez, T., 2002. Source analysis of polyspike and wave complexes in juvenile myoclonic epilepsy. Seizure 11 (5), 320–324.

Scherg, M., 1990. Fundamentals of dipole source potential analysis. In: Grandori, F., Hoke, M., Romani, G. (Eds.), Auditory Evoked Magnetic Fields and Electric Potentials. Karger, Basel, pp. 40–69.

Scherg, M., Ille, N., Bornfleth, H., Berg, P., 2002. Advanced tools for digital EEG review: virtual source montages, whole-head mapping, correlation, and phase analysis. J. Clin. Neurophysiol. 19 (2), 91–112.

Slaght, S.J., Paz, T., Chavez, M., Deniau, J.M., Mahon, S., Charpier, S., 2004. On the activity of the corticostriatal networks during spike-and-wave discharges in a genetic model of absence epilepsy. J. Neurosci. 24 (30), 6816–6825.

Steinhoff, B.J., Racker, S., Herrendorf, G., Poser, S., Grosche, S., Zerr, I., Kretzschmar, H., Weber, T., 1996. Accuracy and reliability of periodic sharp wave complexes in Creutzfeldt–Jakob disease. Arch. Neurol. 53 (2), 162–166.

Traub, R.D., Pedley, T.A., 1981. Virus-induced electrotonic coupling: hypothesis on the mechanism of periodic EEG discharges in Creutzfeldt–Jakob disease. Ann. Neurol. 10 (5), 405–410.

Tschampa, H.J., Herms, J.W., Schulz-Schaeffer, W.J., Maruschak, B., Windl, O., Jastrow, U., Zerr, I., Steinhoff, B.J., Poser, S., Kretzschmar, H.A., 2002. Clinical findings in sporadic Creutzfeldt–Jakob disease correlate with thalamic pathology. Brain 125 (Pt 11), 2558–2566.

Tschampa, H.J., Murtz, P., Flacke, S., Paus, S., Schild, H.H., Urbach,

H., 2003. Thalamic involvement in sporadic Creutzfeldt–Jakob disease: a diffusion-weighted MR imaging study. AJNR Am. J. Neuroradiol. 24 (5), 908–915.
Tschampa, H.J., Kallenberg, K., Urbach, H., Meissner, B., Nicolay, C., Kretzschmar, H.A., Knauth, M., Zerr, I., 2005. MRI in the diagnosis of sporadic Creutzfeldt–Jakob disease: a study on inter-observer agreement. Brain 128 (Pt 9), 2026–2033.
Urbach, H., Klisch, J., Wolf, H.K., Brechtelsbauer, D., Gass, S., Solymosi, L., 1998. MRI in sporadic Creutzfeldt–Jakob disease: correlation with clinical and neuropathological data. Neuroradiology 40 (2), 65–70.
Wieser, H.G., Schwarz, U., Blattler, T., Bernoulli, C., Sitzler, M., Stoeck, K., Glatzel, M., 2004. Serial EEG findings in sporadic and iatrogenic Creutzfeldt–Jakob disease. Clin. Neurophysiol. 115 (11), 2467–2478.
Wieser, H.G., Schindler, K., Zumsteg, D., 2006. EEG in Creutzfeldt–Jakob disease. Clin. Neurophysiol. 117 (5), 935–951.
Zochodne, D.W., Young, G.B., McLachlan, R.S., Gilbert, J.J., Vinters, H.V., Kaufmann, J.C., 1988. Creutzfeldt–Jakob disease without periodic sharp wave complexes: a clinical, electroencephalographic, and pathologic study. Neurology 38 (7), 1056–1060.